Iğdır Üniversitesi Fen Bilimleri Enstitüsü Dergisi, 12(1): 389-402, 2022
Journal of the Institute of Science and Technology, 12(1): 389-402, 2022

ISSN: 2146-0574, eISSN: 2536-4618

Makina Mühendisliği / *Mechanical Engineering* **DOI: 10.21597/jist.952021**

Araştırma Makalesi / *Research Article*

Geliş tarihi / Received: 14.06.2021 **Kabul tarihi / Accepted: 08.10.2021**

To Cite: Yazici MY, 2022. Thermal Management of Small-Scale Li-ion Battery Module Using Graphite Matrix Composite with Phase Change: Effect of Discharge Rate. Journal of the Institute of Science and Technology, 12(1): 389-402.

Thermal Management of Small-Scale Li-ion Battery Module Using Graphite Matrix Composite with Phase Change: Effect of Discharge Rate

Mustafa Yusuf YAZICI[1]*

ABSTRACT: An experimental study is performed to investigate the performance (thermally and electrically) of a small-scale li-ion module (3s2p) using passive thermal management strategy of phase change material (PCM)/graphite matrix. The PCM/graphite matrix was obtained by impregnating the graphite matrix (bulk density: 75 g L-1) with phase change material (paraffin/organic, RT-35). The performance tests of a li-ion module are conducted at 1C and 1.6C discharge rates for graphite matrix composite with phase change (phase change composite or PCM/graphite matrix) and also air cooling, comparatively. To illustrate the performance of the PCM/graphite matrix, transient temperature variations, thermal imaging, discharge capacity, and energy capacity are achieved comprehensively. The results illustrate that graphite matrix composite with phase change has a significant contribution to melting heat transfer, operating temperature, utilized capacity, and energy capacity compared to air cooling. Effective thermal conductivity of PCM/graphite matrix is increased 35 times by comparison with pure paraffin. Operating temperature and temperature gradient throughout the li-ion surface decrease by 22 % and 43 % compared to the air cooling, respectively, for high discharge rate. Operating time and energy capacity is increased 33 % and 28% compared to natural air cooling, respectively, for high discharge rate. It is also disclosed that dominant heat transfer mechanism is conduction depending on micro/nano-size porous structure of graphite matrix.

Keywords: Battery, cooling, graphite, li-ion, phase change material (PCM), thermal management

[1]Mustafa Yusuf YAZICI (**Orcid ID:** 0000-0002-1076-9265), Samsun Üniversitesi, Mühendislik Fakültesi, Makine Mühendisliği Bölümü, Samsun, Türkiye

***Corresponding Author**: Mustafa Yusuf YAZICI, e-mail: myusuf.yazici@samsun.edu.tr

INTRODUCTION

Li-ion batteries among battery technologies are the most promising power sources with no memory effect, lower self-discharge, lower mass density, higher energy density, and stable performance for EVs and also other applications such as electronics, robotics, aerospace, renewable energy sources, etc. One of the major hindrances regarding the li-ion is temperature-caused degradation. There are two main temperature concerns about li-ion batteries: unacceptable operating temperature, low-temperature uniformity. Adverse effects of temperature can be categorized as high temperature-performance degradation, thermal runaway, temperature maldistribution, and low-temperature behavior. The operating temperature of the li-ion battery needs to be kept within an acceptable narrow of 15°C - 35°C for optimum performance. Besides, temperature gradient among cells in the battery pack is desired to be less than 5 °C. Therefore, a well-designed battery thermal management system (BTMS) is required to ensure better battery performance and safety during charge/discharges (Liu et al., 2017; Landini et al., 2019; Zichen and Changqing, 2021).

BTMS through phase change material (PCM, solid/liquid) is an attractive way due to high energy storage capability and isothermally process. Besides, a PCM-based battery thermal management system ensures minimizing the complexity and providing weight, volume, power consumption, and noise. Nevertheless, thermal conductivity and leakage issues of PCM-based thermal management strategies for organic paraffin type are two main bottlenecks restricting usage of PCM-based technology. Lower thermal conductivity results in lower heat transfer rates and longtime solid/liquid phase transition process. Besides, form stable is not provided during the melting period. So, it requires encapsulation of PCM. This weakness of material depending on its nature can be improved using different methods investigating by researchers including increasing the heat transfer area (Aydin et al., 2018), geometric optimization (Yazici et al, 2014), dispersing particles (Arshad et al., 2020), metal matrix (Alhusseny et al., 2020), impregnated graphite foam/matrix (Py et al., 2001), encapsulation (Zhang et al., 2021).

Graphite matrix has an increasing research interest with its potential of high thermal conductivity thermal paths for heat dissipation and also encapsulation for preventing leakage issues. Graphite matrix achieves very low density, high porosity, high ratio heat transfer surface to volume, closest thermal conductivity to natural graphite, chemically non-reactive, and good mechanical properties. On the other side, the graphite matrix provides a porous medium for encapsulation. The liquid PCM is saturated/ impregnated to the graphite matrix with the phenomena of surface tension and capillarity. To form shape-stabilized PCMs, impregnation encapsulation is shown to be a potential method by researchers (Zhang et al., 2021). This provides PCM to retain solid phase form without any leakage during melting.

Researches on thermal management of li-ion considering a PCM / graphite matrix-foam to ensure reliable operating temperatures are presented. Mills et al. (2006) first reported (within the authors' knowledge) an expanded graphite matrix for battery cooling. They revealed the potential of the PCM composite for passive thermal management systems. Kızılel et al. (2008) investigated the effect of the PCM/graphite matrix over conventional active cooling systems. The results showed that the surface temperature was lower when PCM was used. A numerical study was conducted to investigate the cooling performance of graphite matrix composite with phase change by Kizilel et al. (2009). Somasundaram et al. (2012) carried out a numerical study for cylindrical li-ion at different discharge currents. The results showed that lower temperature measurements were observed with a PCM/graphite. The thermal performance of composite PCM-based BTMS was performed by Greco et al. (2015). They observed that the relation between thermal conductivity and heat of fusion (latent heat) was significant. The authors also presented that the bulk density of the graphite matrix was a critical parameter for optimizing the

PCM/graphite matrix BTMS. Wilke et al. (2017) investigated the effect of the solid-liquid phase change composite (PCM/graphite matrix) on the thermal runaway for a single cell. Jiang et al. (2016) performed an experimental and numerical study on PCM-based battery thermal management. The expanded graphite-based phase change composite (EG/PCM slurry) was packed in aluminum tubes to improve the heat transfer via thermal conductivity. Wu et al. (2016) studied the effect of a copper mesh-enhanced paraffin/expanded graphite for thermal management of li-ion. Heat dissipation performance and temperature uniformity in better are provided in a better way by this method. A heat pipe-assisted PCM/EG-based BTMS was investigated by the same research group (Wu et al., 2017). Mallow et al. (2018) studied aluminum and graphite foam composites via saturation of PCM. He et al. (2019) developed composite PCM by introducing a thermal conductive skeleton of EG/copper foam for BTMS.

Because the li-ion battery is promising and updated technology in terms of an anode, cathode, electrolyte, etc., researches on thermal management are renewed by authors. From the cited literature, there are some studies on PCM/graphite matrix or foam for different li-ion chemistries or simulative batteries under various loading conditions. However, it is shown that the researches are needs to be expanded. Therefore, the goal of this study is to evaluate the effect of the phase transition phenomenon and porous media of PCM/graphite matrix on the heat dissipation process for battery thermal management, which is essential for better performance and safety requirements. Transient temperature recordings and thermal images are utilized under different discharge rates to illustrate the melting phase transition phenomenon and thermal energy storage behavior of graphite matrix composite with phase change. The electrical performance of the li-ion is presented by the way discharge and energy capacity variation. Free air cooling is also performed compared to the PCM/graphite matrix.

MATERIALS AND METHODS

Phase change material and phase change composite (PCM/graphite matrix)

As a heat storage material, organic-paraffin (RT35-Rubitherm) was used in this study. Paraffin has significant potential for heat absorption with its advantages including, high latent heat of fusion, stability in chemical/thermal, compatibility with materials, no phase segregation. The thermophysical properties of the paraffin and phase change composite (PCM/graphite matrix) are given in Table 1. Heat flow of materials was reported by DSC analysis (Hitachi-DSC 7020) in Figure1.

Table 1. Thermo-physical properties of the pure paraffin and phase change composite

Thermo-physical property	Pure paraffin	Phase change composite
Melting temperature (°C)	37.2	36.1
Latent heat (kJ kg^{-1})	150	144
Thermal conductivity (W m^{-1} K^{-1})	0.2	7.2
Density (kg m^{-3}) (at 25 °C)	860	796

The graphite matrix was made by compacting expanded graphite (EG) to the desired bulk density. EG was achieved by rapid expansion and exfoliation of expandable graphite in a furnace over 900 °C for 60 seconds. A detailed description of the process of expanded graphite is presented in literature (Mills et al., 2006). For this investigation, expandable graphite (>%98 purity, 50 mesh, and 700 ml g^{-1}) was supplied by Asbury Carbon, and EG was provided by heat treatment. Then, EG granules were compressed by a universal testing system (Instron 3382) to a bulk density of 75 g L^{-1} graphite matrix.

Graphite matrix with an overall dimension of 75mm x 52mm x 60mm (length x width x height) was manufactured for lower scale battery pack configuration (3s2p). The graphite matrix prepared for lower scale battery pack configuration was submerged in a melted paraffin bath (70°C) for about 4 hours

to complete saturation for producing PCM/graphite matrix composite. The graphite matrix was saturated with phase change material via capillary forces (Py et al., 2001; Mills et al., 2006). Here, it should be impressed that capillary forces prevent PCM leakage to the outside during phase transition. The total amount of PCM in the phase change composite of PCM/graphite matrix was 112.88 grams. The mass fraction of paraffin is about 92% in phase change composite. The porosity of the EG matrix was computed, approximately, 85% by using PCM volume in the matrix.

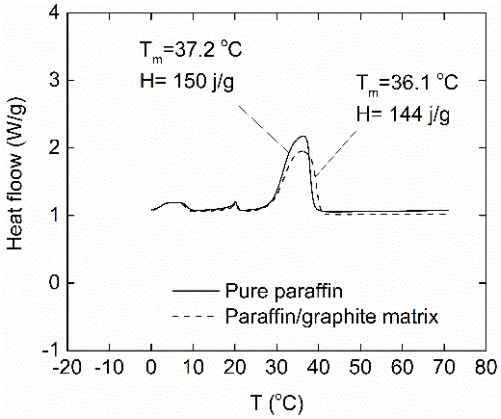

Figure 1. Heat flow-temperature variation for pure paraffin and paraffin/graphite

Scanning electron microscope (SEM) photographs of the graphite matrix and the phase change composite with different modes of SEM, the backscattered electrons (BSE), and the secondary electron (SE) are presented in Figure 2. SE modes (Figure 2a, c) are very useful for the inspection of the topography of the sample's surface. On the other side, BSEs (Figure 2b, d) are used to detect contrast between areas with different chemical compositions. It is shown that the compacted expanded graphite matrix exhibits vermicular particles (Figure 2a). There are some regions, which do not interlock each other in the EG matrix in Figure 2a. The honeycomb-like network is occurred due to the overlapping and intersecting of graphite flakes (Figure 2a) (Zou et al., 2020). The black areas seen in Figure 2b displays non-interlocking areas. Figure 2c presents the morphology of the EG matrix covered with paraffin (phase change composite). It can result in that paraffin of high amount is impregnated to pores of EG layers. Figure 2d clearly shows the different chemical phases between PCM and graphite.

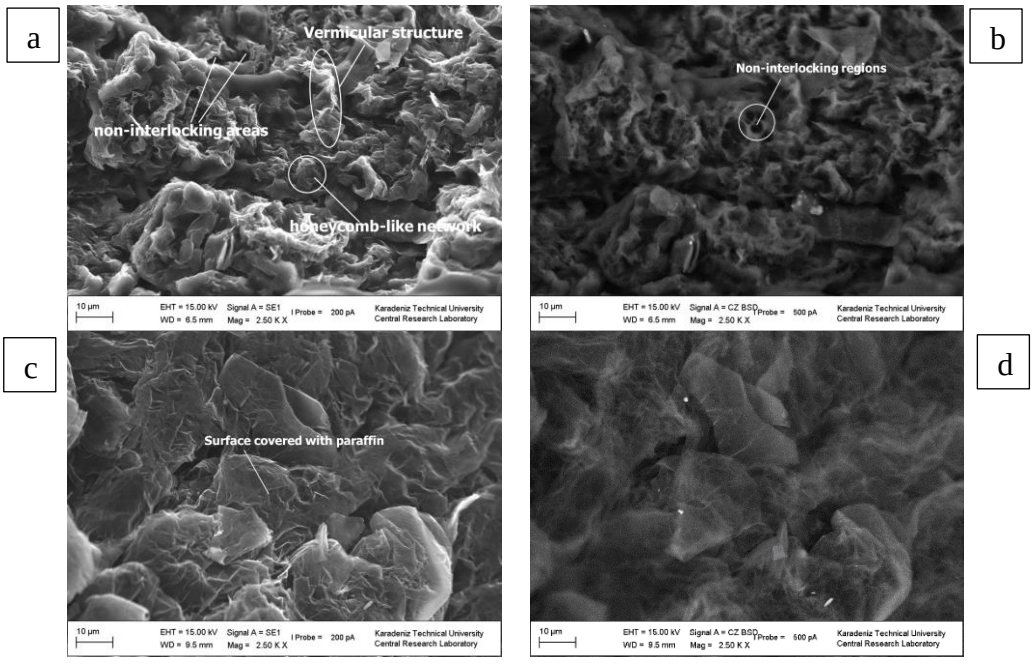

Figure 2. SEM photographs: SE and BSD modes of the graphite (a,b) and phase change composite (c,d)

Optical images indicating leakage test results of phase change composite sample are illustrated in Figure 3. The graphite/PCM matrix composite sample was placed on paper and heated at 75 °C for 150 minutes PCM/graphite matrix keeps its form with a very low amount of leakage < 0.42 gram on paper. The leakage mass percentage of the composite is 0.37 %. These low amounts of leakage are explained by the melting of the surface solidified PCMs.

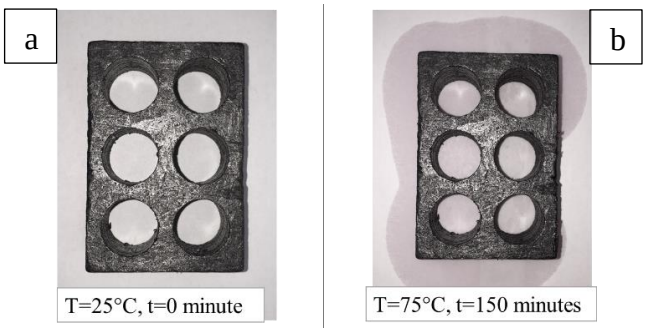

Figure 3. The leakage test result of phase change composite; T=25°C (a), T=75°C (b)

Experimental procedure

The experimental facility built to evaluate the effect of graphite matrix composite with phase change (phase change composite or PCM/graphite matrix) on battery thermal management is illustrated in Figures 4 and 5. It consists of five main parts: test section (PCM/graphite matrix or air cooling), electronic dc load, data logger, thermal camera, and PC.

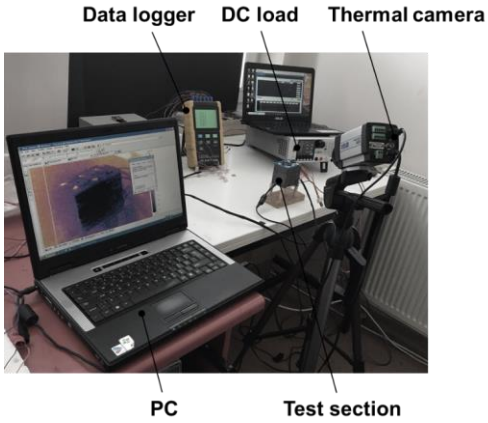

Figure 4. Experimental setup

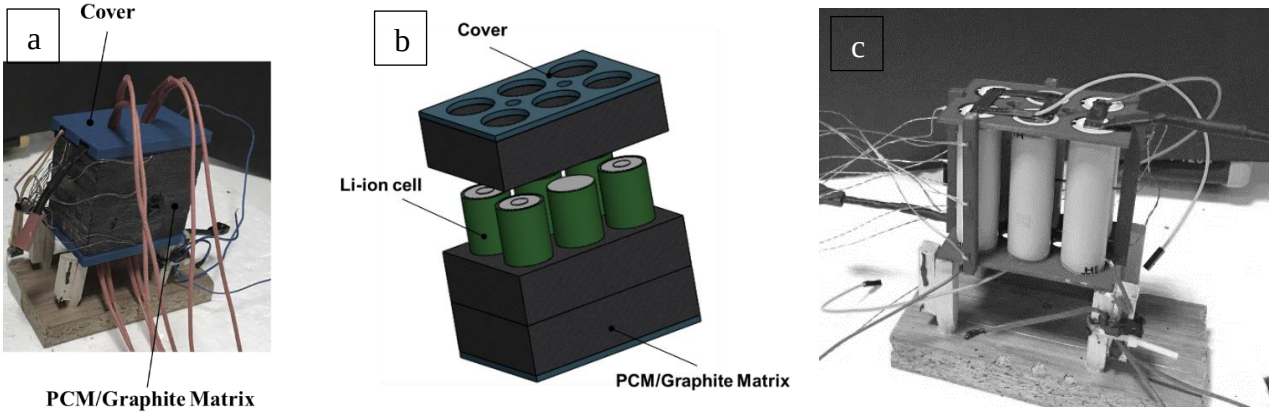

Figure 5. Test section: phase change composite /photograph (a), phase change composite /shematic view (b), air cooling/photograph (c)

The construction details of the test section are shown in Figure. 5. Test section comprises li-ion cell (3s2p), and PCM/graphite matrix/air cooling arrangements. A commercially available li-ion cell

(Panasonic-Sanyo NCR 18650B) was used in the test module. The specifications of the battery module are shown in Table 2.

Table 2. Li-ion cell/pack specification

Specification	cell	module
Form factor	1s	3s2p
Capacity nominal (mA h)	3350	6700
Voltage nominal (V)	3.7V	11.1
Specific energy (W h kg^{-1})	243	258

To monitor the temperature response along with the li-ion cell, six thermocouples of T-type supplied by OMEGA (T_{1-6}) with an accuracy of ±1 °C (or 0.75% whichever greater) were placed on the two li-ion cells (cell 1 and cell 2). The thermocouple locations on both cells are shown in Figure 6. A thermal camera (Flir/ thermovision series) was also used to visualize the thermal image of both air-cooling and phase change composite (PCM/graphite matrix) arrangements. Transient temperature measurements were recorded with the accuracy of ± % 0.5 F.S. (± 2.1°C). via a data logger system (PCE-1200) by 5 seconds intervals. The li-ion module was discharged at 1.6C-rate (10 Amper) using a Chroma electronic dc load (CH-63004). For constant current mode of dc load, the measurement accuracy of current is ± 0.1 % F.S. (±0.06 amper)

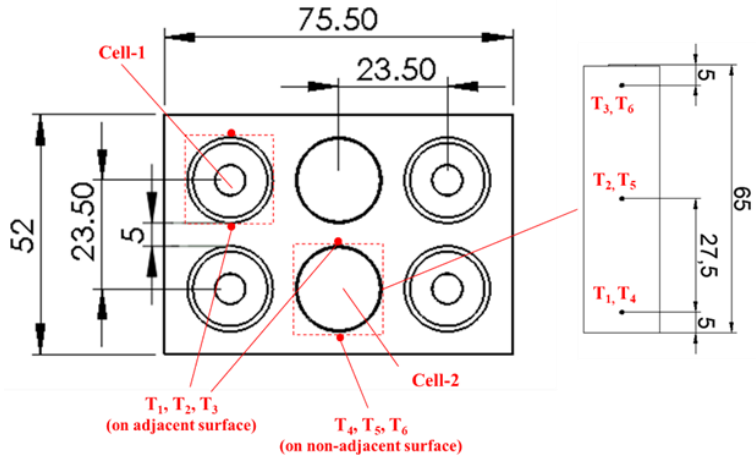

Figure 6. The points of the temperature measurements on the Li-ion cell

All the experiments of air cooling and PCM/graphite matrix were carried out in a conditioned room, where the ambient temperature is 25°C. Experiments were terminated by reaching the limit operating temperature (55°C) or cut-off voltage (2.5 V) value whichever comes first. By following the approach of Kline & McClintock, the combined uncertainty of each measurement is found to be ±0.9%.

RESULTS AND DISCUSSION

The effect of the PCM/graphite matrix on the thermal management of the li-ion module (3s2p) is tested experimentally compared to the reference case of natural air cooling. Experiments are carried out at room temperature for 1C and 1.6C rates. The time history of temperature (T °C) variations at six local temperature points for two cells (cell 1 and cell 2) and the thermal images are presented in Figure 7-8 and Figure 10-11 to evaluate the thermal performance of each battery pack arrangement for 1.6C rate and 1C rate, respectively. The voltage (V)-discharge capacity (A h) variation and energy capacity (Watt hour: W h) is also given in Figure 9 and Figure 12 to reveal the electrical performance of each battery pack for 1.6C-rate and 1C-rate, respectively.

Heat transfer through expanded graphite matrix, which is attractive material depending on its including properties including very low density, high porous structure, high heat transfer surface to volume ratio, is occurred with abundant thermal paths, which are highly conductive. This results in rapid heat dissipation on the EG matrix. These advantages of the expanded graphite matrix speed up the process of diffusing and storing heat in the PCM. Heat transportation mechanism in such porous medium results by conduction (Mills et al., 2006; Kang et al., 2019). The free convection heat transfer does not occur within pores smaller than 10 mm (Kang et al., 2019). SEM images confirm that pore sizes are in micro-scale for graphite matrix structure in Figure 2. Therefore, conduction heat transfer is the only mechanism for heat transport in the PCM/graphite matrix structure.

Experimental results for 1.6C

Temperature profiles of each battery pack configuration tested at the 1.6C rate are shown in Figure 7. For the natural air-cooling case, surface temperatures of the li-ion cell increase steeply with time in Figure 7a-b. For air cooling, the heat dissipated from the outer surface of the li-ion cell is not transferred effectively by air cooling due to the low thermal conductivity (0.025 W m^{-1} K^{-1} at 25°C) and also low natural convection rates. This behavior causes reaching the limit operating temperature (55 °C) in a shorter time of 24 minutes. It is shown from Figure 7a-b that the local temperature points of $T_{1\text{-}3/cell\text{-}1}$ and $T_{1\text{-}3/cell\text{-}2}$, which are positioned on adjacent surfaces facing each other, have higher temperature measurements. In addition, cell-2 temperature history is higher (1-3 °C) than cell-1. These are a result of the thermal effect caused by neighboring batteries surrounding the cell-2 battery. Hence, a non-uniform temperature profile along with the cell ($T_{maximum}$-$T_{minimum}$=$T_{3/cell\text{-}2}$-$T_{4/cell\text{-}1}$=7 °C) occurred more specifically. However, for the phase change composite (PCM/graphite matrix), the increment rate of the surface temperature is lower than the natural air cooling (Figure 7c-d). Also, a more uniform temperature gradient is observed by the PCM/graphite matrix. This is the result of the considerable increase of heat dissipation rates throughout the li-on cell surfaces to the medium and the thermal energy storage capacity of PCM. The higher heat dissipation rate due to abundant thermal paths provides a higher heat transfer rate. Dissipated heat in the phase change composite (PCM/graphite matrix) is absorbed by paraffin in the form of sensible (period of temperature increasing) and latent heat (period of phase transition). It is shown in Figure 7c-d that temperature measurements report a steep increase in the first period of discharging due to sensible heat storage (Figure 7c-d, t < 4 minutes). In the next period, it is shown from Figure 3c-d that temperature values along the li-ion cells reach the melting area of RT-35 ($T_{melting}$=29°C-36°C), and a positive decreasing variation during the solid-liquid phase transition occurs depending on latent heat of fusion, which has a high energy storage capacity (Figure 7b, 4 minutes< t < 25 minutes). In this period, latent heat storage is the dominant energy storage mechanism. In the following stage (Figure 7c-d, t > 25 minutes), the rate of temperature increase again advances, because the phase change process is completed. For example, at=24 minutes, it is seen from Figure 7b and d that recorded maximum surface temperatures are 55 °C ($T_{3/cell\text{-}2}$) and 43 °C ($T_{3/cell\text{-}2}$) for natural air cooling and PCM/graphite matrix, respectively. On the other side, the maximum surface temperature difference decreased to the value of 4 °C ($T_{maximum}$-$T_{minimum}$= $T_{3/cell\text{-}2}$- $T_{5/cell\text{-}1}$) by PCM/graphite matrix. Temperature differences between both cell2-cell1 and on adjacent ($T_{1,2,3)}$-nonadjacent ($T_{4,5,6}$) surfaces compensated depending on high thermal diffusivity medium compared to air cooling. These outputs reveal that for the PCM/graphite matrix, operating temperature and temperature difference on the li-ion surface are approximately 22 % and 43 % lower compared to natural air cooling, respectively. Therefore, the PCM/graphite matrix also provides a longer operating time in reliable operating temperatures. It is shown from Figure 7c-d that operating time in reliable temperature ranges increases up to 32 minutes

with an increase of 33 % compared to natural air cooling. It should be remembered that experiments are terminated with reaching the limit operating temperature (55 °C) or cut-off voltage (7.8 V) value whichever comes first. For natural air cooling and PCM/graphite matrix, operating temperature and cut-off voltage value were observed as a limit experimental condition, respectively.

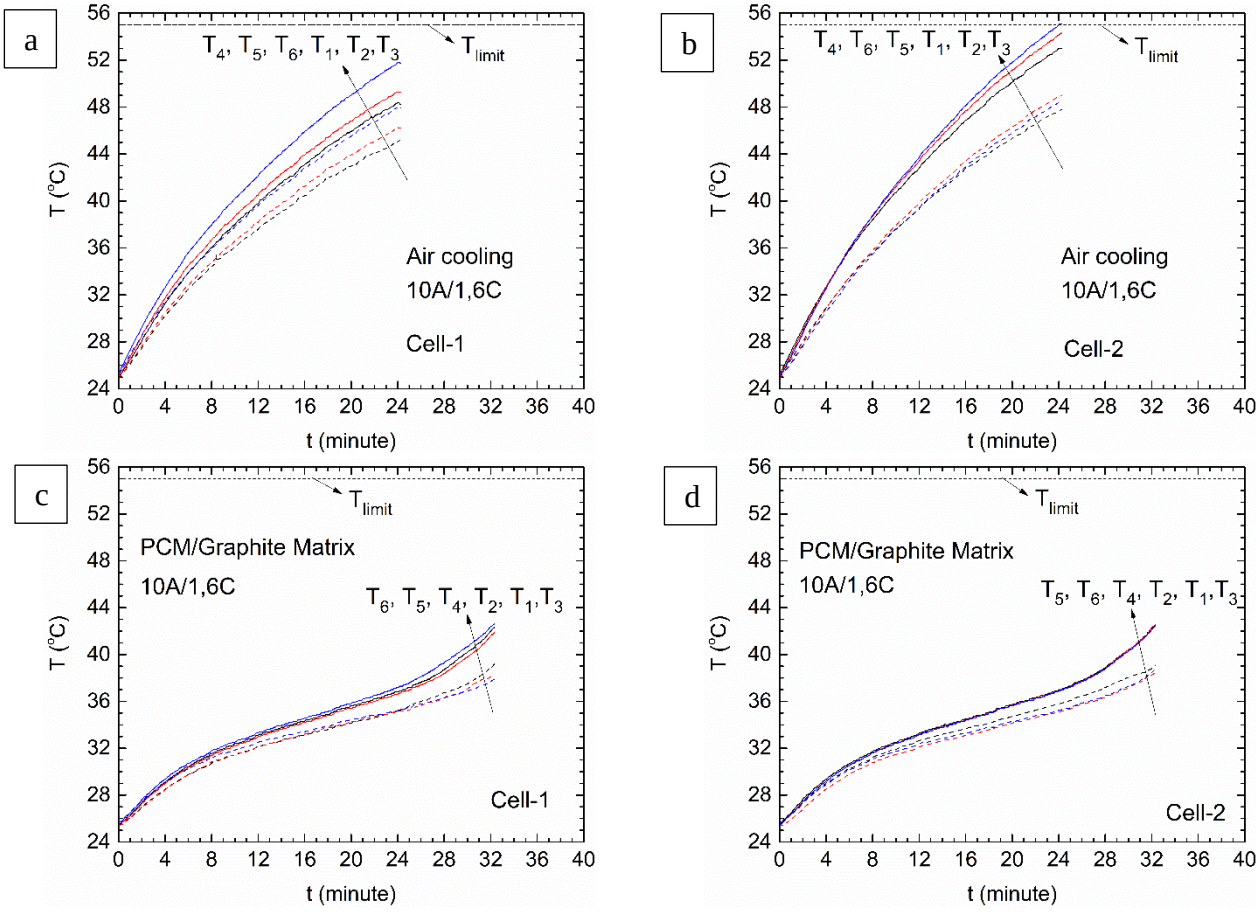

Figure 7. The time history of temperature along the li-ion cell surface: natural convection case (a, b), the PCM/graphite matrix (c,d)

Temporal thermal camera images are presented every ten minutes in Figure 8. The last thermal images of both configurations are at the time of reaching the limit condition at which the experiment is completed. It is shown that the temperature increment rate is faster for natural air cooling compared to the PCM/graphite matrix. For the final period of the experiment, the increment rates of temperature (from $T_{initial}$ to T_{final}) are 116% and 66% for air cooling and PCM/graphite matrix, respectively. Besides, temperature increment rates are 1.2 °C minutes^{-1} and 0.51 °C minutes^{-1} for air cooling and PCM/graphite matrix under 1.6C rate, respectively. Here, it should be emphasized that thermal images in Figure 8b present temperature contours of PCM/graphite matrix outer surface. It is observed that outer (Figure 8b) and inner (Figure 7c/d) surface temperature measurements of the PCM/graphite matrix are close to each other. This behavior evaluates the higher thermal diffusivity and higher heat transfer rates radially and axially. The temperature field on the li-ion cell surface for natural air cooling and phase change composite (PCM/graphite matrix) supports Figure 7, which belongs to thermocouple measurements.

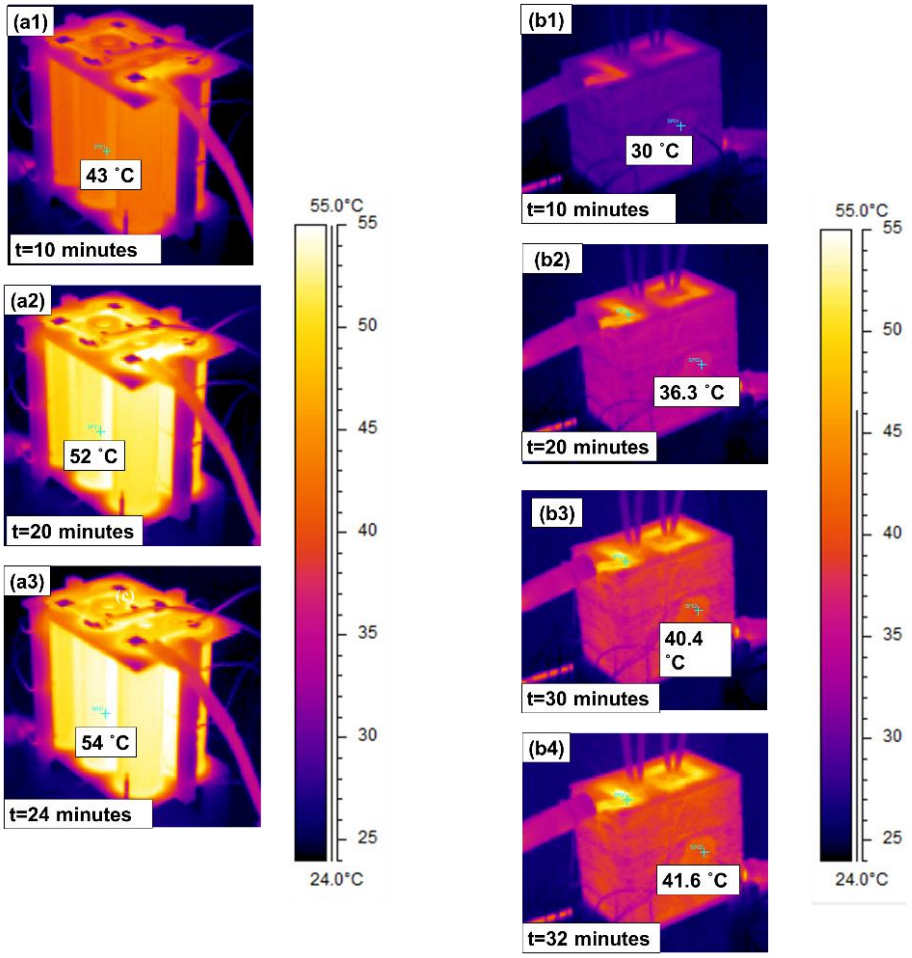

Figure. 8. Transient thermal camera images: natural (free) convection, li-ion surface (a), PCM/graphite matrix (outer surface) (b)

Electrical performance findings of discharge capacity and energy capacity for each battery pack configuration are given in Figures 9 and 10. It is shown from the Figure 9 that utilized capacity (discharge capacity) values are 4 A h (Amper hour) and 5.5 A h (Amper hour) for natural air cooling and phase change composite (PCM/graphite matrix), respectively. It should be expressed that the utilized capacity of the battery module using the PCM/graphite matrix, which is higher 38% than natural air cooling, is achieved at a reliable operating temperature/voltage range. However, the voltage decrement rate is slightly lower for the air-cooling case. This can be explained by higher temperature measurements on the package, which provides higher ionic conductivity for air cooling. On the other side, reaching the limit of the surface temperature of 55 ˚C inhibits the longer-duration use and more capacity usage of a cell. Another electrical performance finding of energy capacity (Watt hour: W h) variation for both cases is presented in Figure 10. It is illustrated in Figure 10a that the battery module with PCM/graphite matrix delivers to 51 W h (Watt hour) with a linear increment, approximately, 28% more power compared to air cooling (40 W h) for an hour. This behavior evaluates that more amount of work performed is obtained by the case of PCM/graphite matrix cooling under reliable operating conditions. The reached total energy capacity is also presented comparatively in column chart format.

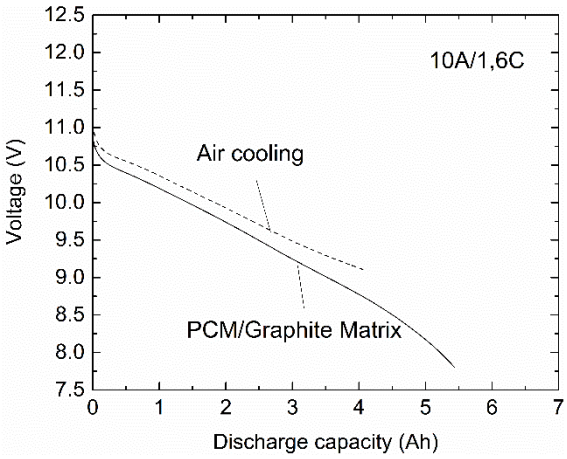

Figure 9. Capacity-voltage variation during discharge

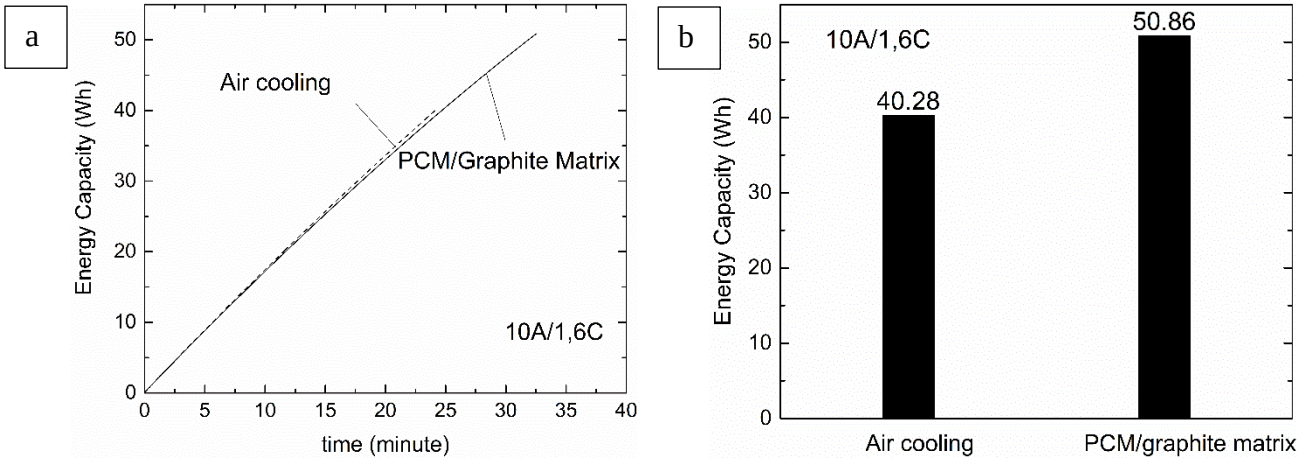

Figure 10. Energy capacity variation during discharge for different cooling strategies: time history of energy capacity (a), total energy capacity value (b)

Experimental results for 1C

Temperature histories for a lower discharge rate of 1C are presented in Figure 11. It is shown that lower local temperature measurements are recorded with a similar variance trend with the 1.6C rate. For example, at t=24 minutes, temperature measurements are 38°C ($T_{maximum}=T_{3/cell-2}$, air cooling), 32°C ($T_{maximum}=T_{3/cell-2}$, PCM/graphite matrix) for 1C rate; 55°C ($T_{maximum}=T_{3/cell-2}$, air cooling), 37°C ($T_{maximum}=T_{3/cell-2}$, PCM/graphite matrix) for 1.6C rate, respectively. These measurements result in the maximum temperature value of air cooling is 19% higher than PCM/graphite matrix under 1C rate. Besides, for the 1C rate (Figure 11c, d), temperature values of air cooling (Figure 11a, b) and PCM/graphite matrix is 31% and 14% lower, respectively, compared to the 1.6C rate. However, for the natural air-cooling case, after the period of rapid increase of temperature (t>8 minutes), the rate of temperature rise is decreasing depending on the natural convection heat transfer mechanism. In the following period (t>56 minutes), the rate of temperature rise is increasing again because of insufficient natural air cooling. On the other side, the battery pack with PCM/graphite matrix has lower temperature recording, but it is not observed rapid temperature increment for the second time after the completion of phase transition. This is a result of the reaching only upper limit of the phase transition temperature. In another word, the phase transition is just completed or is going on. Cut-off voltage value was observed as a limit experimental condition for both natural air cooling and PCM/graphite matrix for 1C rate. Reliable operating time is observed 60 minutes and 57 minutes for air cooling and PCM/graphite matrix,

respectively. This is the result of the higher operating temperatures, which provide higher ionic conductivities for air cooling configuration.

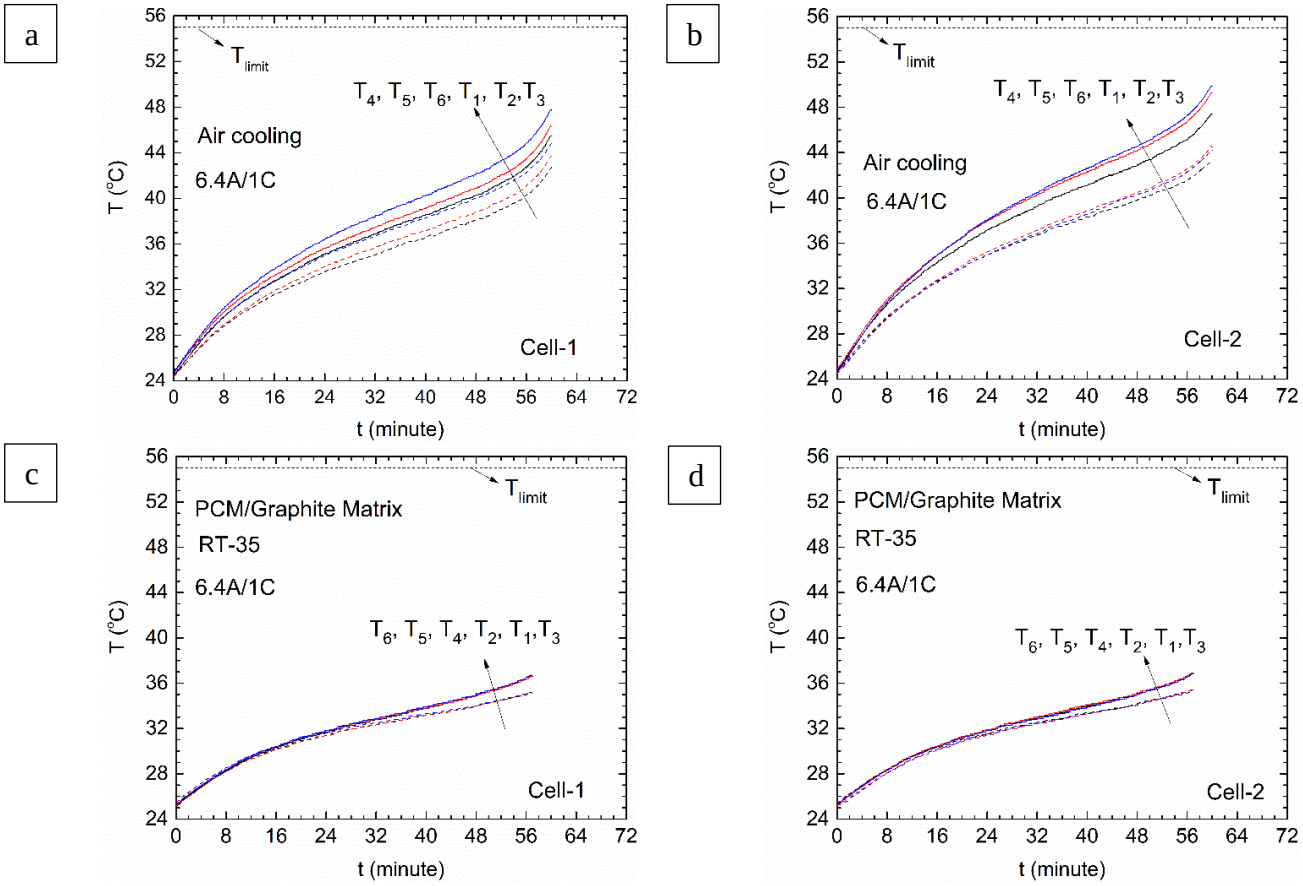

Figure 11. The time history of temperature along the li-ion cell surface: natural air convection case (a, b), the PCM/graphite matrix (c, d)

Transient thermal images of 1C rate are given every ten minutes for air cooling and PCM/graphite matrix in Figure 12. For the final period of the experiment, the increment rates of temperature (from $T_{initial}$ to T_{final}) are 118% and 35% for air cooling and PCM/graphite matrix, respectively. Besides, temperature increment rates are 0.5 °C minutes $^{-1}$ and 0.17 °C minutes $^{-1}$ for air cooling and PCM/graphite matrix under 1C rate, respectively. These values are nearly half of the values of the 1.6C-rate. It is observed that outer (Figure 12b) and inner (Figure 11c, d) surface temperature values of the PCM/graphite matrix are close to each other. The temperature field on the li-ion cell surface for natural air cooling and PCM/graphite matrix support Figure 11, which belongs to thermocouple recordings.

Discharge capacity-voltage and energy capacity histories are shown for each battery pack configuration Figure 13 and 14, respectively. It is shown that utilized capacity values are 6.4 A h (Amper hour) and 6.1 A h (Amper hour) for natural air cooling and PCM/graphite matrix, respectively. There is a slight difference of 5% in the value of utilized capacity. For air cooling configuration, utilized capacity is higher depending on higher temperature measurements on the package, which provides higher ionic conductivity for air cooling. Energy capacity variation is also presented in Figure 14. Time history of energy capacity variation shows similar curve characteristics with a high discharge rate. However, unlike the 1.6C-rate, the energy capacity value reaches slightly higher values for air cooling under 1C-rate. This slight difference of 6.6% supports the higher capacity usage depending on the operating temperature of the li-ion module with air cooling. The total energy capacities are nearly 64 W h (Watt hour) and 60 W h (Watt hour) for air cooling and PCM/graphite matrix configurations, respectively, in Figure 14b.

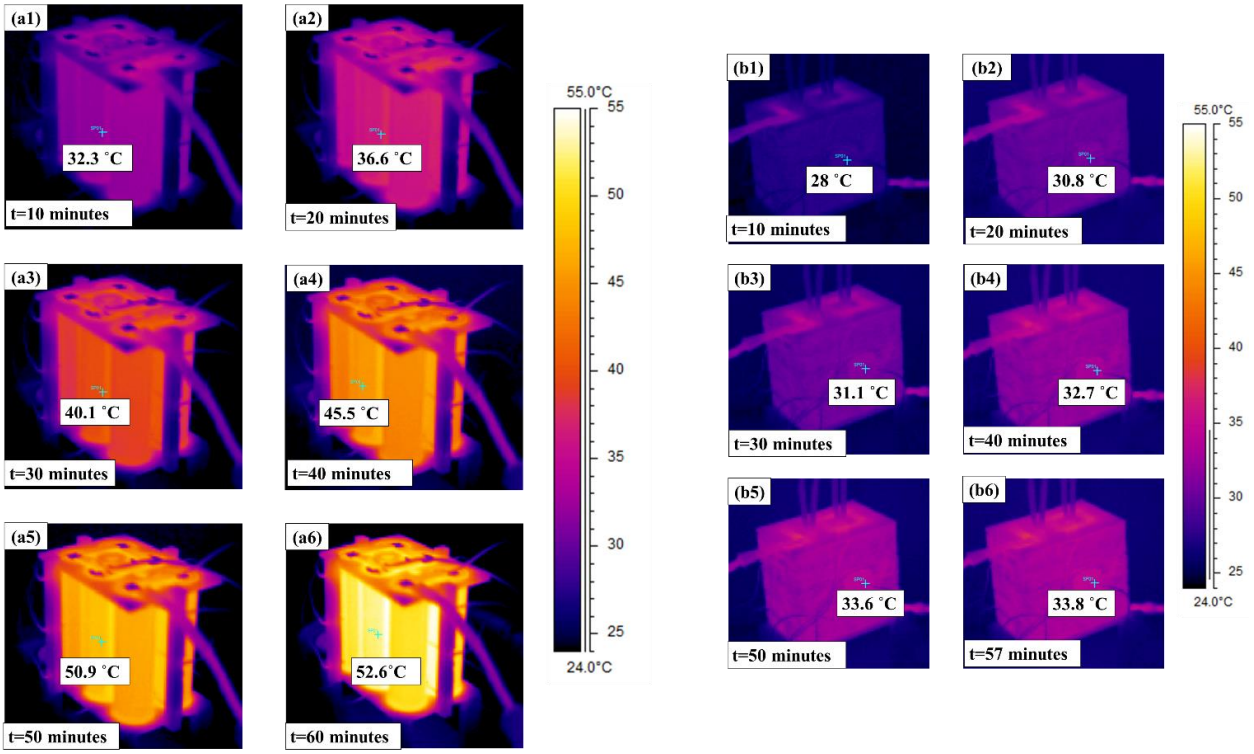

Figure 12. Transient thermal camera images at 1C rate: natural convection, li-ion surface (a), PCM/graphite matrix (outer surface) (b)

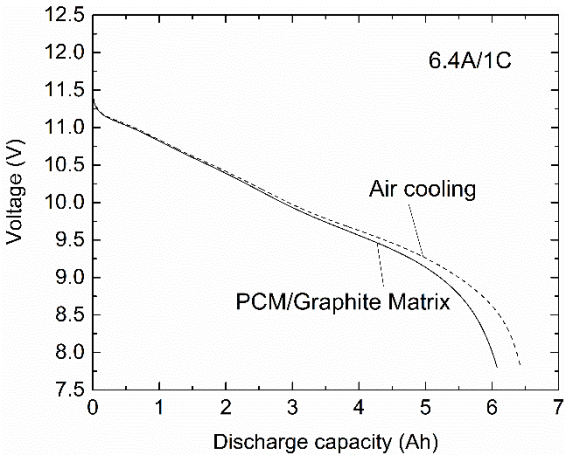

Figure 13. Capacity-voltage variation during discharge

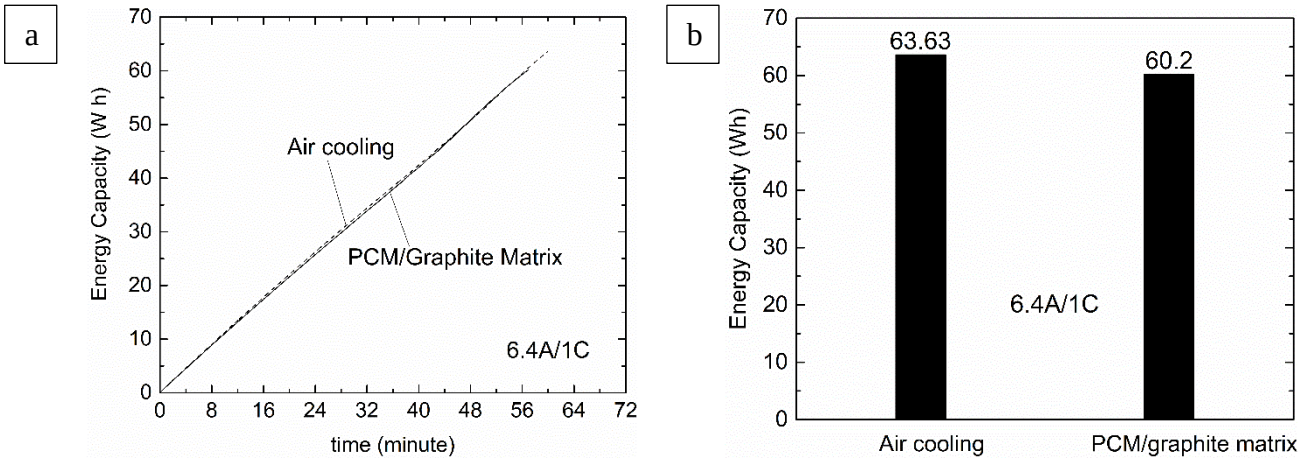

Figure 14. Energy capacity variation during discharge for different cooling strategies: time history of energy capacity (a), total energy capacity value (b)

CONCLUSION

In this study, the effect of PCM/graphite matrix on li-ion battery thermal management is carried out experimentally. The results reveal that the PCM/graphite matrix has significant potential in battery thermal control systems, especially, for higher discharge rates. The temperature is successfully regulated and distributed uniformly in the li-ion module. The main conclusions may be summarized as follows:

- For the PCM/graphite matrix, operating temperature and temperature gradient on the li-ion module is decreased by 22 % and 43 %, respectively for the 1.6 °C-rate.
- For the PCM/graphite matrix, the operating time within safe temperature limits is increased 33 % compared to natural air cooling for the 1.6C-rate.
- For the PCM/graphite matrix, the utilized capacity, and energy capacity are increased by 38% and 28%, respectively, compared to natural air cooling for the 1.6C-rate.
- The PCM/graphite matrix configuration is more effective for higher discharge rates (1.6C).
- For lower discharge rates (1C), there is no significant difference in performance for air cooling and graphite matrix composite with phase change.
- The leakage issue was avoided by graphite matrix, which is the way of impregnated encapsulation via capillarity.
- For the graphite matrix composite with phase change, conduction is the main heat transportation mechanism.

ACKNOWLEDGMENT

This study was financially supported by TUBITAK TEYDEB with project number 2180111.

REFERENCES

Alhusseny A, Al-Zurfi N, Nasser A, Al-Fatlawi A, Aljanabi M, 2020. Impact of using a PCM-metal foam composite on charging/discharging process of bundled-tube LHTES units. International Journal of Heat and Mass Transfer, 150: 119320.

Arshad A, Jabbal M, Yan, Y, 2020. Thermophysical characteristics and application of metallic-oxide based mono and hybrid nanocomposite phase change materials for thermal management systems. Applied Thermal Engineering, 181: 115999.

Aydin O, Avci M, Yazici MY, Akgun M, 2018. Enhancing storage performance in a tube-in shell storage unit by attaching a conducting fin to the bottom of the tube. Isı Bilimi ve Teknigi Dergisi-Journal of Thermal Science And Technology, 38(2): 1-13.

Greco A, Jiang X, Cao D, 2015. An investigation of lithium-ion battery thermal management using paraffin/porous-graphite-matrix composite. J. Power Sources, 278: 50–68.

He J, Yang X, Zhang G, 2019. A phase change material with enhanced thermal conductivity and secondary heat dissipation capability by introducing a binary thermal conductive skeleton for battery thermal management. Applied Thermal Engineering, 148: 984-991.

Jiang GW, Huang JH, Fu YS, Cao M, Liu MC, 2016. Thermal optimization of composite phase change material/expanded graphite for li-Ion battery thermal management. Thermal Engineering, 108: 1119-1125.

Kang S, Choi JY, Choi S, 2019. Mechanism of heat transfer through porous media of inorganic intumescent coating in cone calorimeter testing. Polymers, 11(2): 1-16.

Kizilel R, Lateef A, Sabbah R, Farid MM, Selman JR, Al-Hallaj S, 2008. Passive control of temperature excursion and uniformity in high-energy Li-ion battery packs at high current and ambient temperature. Journal of Power Sources, 183(1): 370-375.

Kizilel R, Sabbah R, Selman JR, Al-Hallaj S, 2009. An alternative cooling system to enhance the safety of Li-ion battery packs. Journal of Power Sources, 194(2): 1105-1112.

Landini S, Leworthy J, O'Donovan TS, 2019. A review of phase change materials for the thermal management and isothermalisation of lithium-ion cells. Journal of Energy Storage, 25: 100887.

Liu H, Wei Z, He W, Zhao J, 2017. Thermal issues about Li-ion batteries and recent progress in battery thermal management systems: A review. Energy Conversion and Management, 150: 304-330.

Mallow A, Abdelaziz O, Graham S, 2018. Thermal charging performance of enhanced phase change material composites for thermal battery design. Int. J. Thermal Science, 127: 19-28.

Mills A, Farid M, Selman JR, Al-Hallaj S, 2006. Thermal conductivity enhancement of phase change materials using a graphite matrix. Thermal Engineering, 26(14-15): 1652-1661.

Py X, Olives R, Mauran S, 2001. Paraffin/porous-graphite-matrix composite as a high and constant power thermal storage material. Int. J. Heat Mass Transfer, 44(14): 2727–2737.

Somasundaram K, Birgersson E, Mujumdar AS, 2012. Thermal–electrochemical model for passive thermal management of a spiral-wound lithium-ion battery. Journal of Power Sources, 203: 84-96.

Wilke S, Schweitzer B, Khateeb S, Al-Hallaj S, 2017. Preventing thermal runaway propagation in lithium-ion battery packs using a phase change composite material: an experimental Study. J. Power Sources, 340: 51-59.

Wu W, Yang X, Zhang G, Ke X, Wang Z, 2016. An experimental study of thermal management system using copper mesh-enhanced composite phase change materials for power battery pack. Energy, 113: 909-916.

Wu W, Yang X, Zhang G, Chena K, Wang S, 2017. Experimental investigation on the thermal performance of heat pipe-assisted phase change material-based battery thermal management system. Energy Conversion and Management, 138: 486-492.

Yazici MY, Avci M, Aydin O, 2014. Effect of eccentricity on melting behavior of paraffin in a horizontal tube-in-shell storage unit: An experimental study. Solar Energy, 101: 291-298.

Zhang S, Feng D, Shi L, Wang L, Jin Y, 2021. A review of phase change heat transfer in shape-stabilized phase change materials (ss-PCMs) based on porous supports for thermal energy storage. Renewable and Sustainable Energy Reviews, 135: 110127.

Zichen W, Changqing D, 2021. A comprehensive review on thermal management systems for power lithium-ion batteries. Renewable and Sustainable Energy Reviews, 139: 110685.

Zou T, Liang X, Wang S, Gao X, Zhang Z, Fang Y, 2020. Effect of expanded graphite size on performances of modified CaCl2·6H2O phase change material for cold energy storage. Microporous and Mesoporous Materials, 305: 110403.